



Prompt Jpsi and $b \rightarrow J\psi X$ production in pp collisions

P. Robbe

► To cite this version:

P. Robbe. Prompt Jpsi and $b \rightarrow J\psi X$ production in pp collisions. Workshop on Discovery Physics at the LHC, Dec 2010, Mpumalanga, South Africa. pp.1-6. in2p3-00579422

HAL Id: in2p3-00579422

<https://hal.in2p3.fr/in2p3-00579422>

Submitted on 7 Apr 2011

HAL is a multi-disciplinary open access archive for the deposit and dissemination of scientific research documents, whether they are published or not. The documents may come from teaching and research institutions in France or abroad, or from public or private research centers.

L'archive ouverte pluridisciplinaire **HAL**, est destinée au dépôt et à la diffusion de documents scientifiques de niveau recherche, publiés ou non, émanant des établissements d'enseignement et de recherche français ou étrangers, des laboratoires publics ou privés.

Prompt J/ψ and $b \rightarrow J/\psi X$ production in pp collisions

Patrick Robbe^{*†}

LAL, Université Paris-Sud, CNRS/IN2P3, Orsay, France

E-mail: robbe@lal.in2p3.fr

The LHCb measurement of the J/ψ production cross-section is presented. The double differential cross-section is measured as a function of the J/ψ transverse momentum p_T and of the J/ψ rapidity y in the fiducial region $p_T \in [0; 14] \text{ GeV}/c$ and $y \in [2.0; 4.5]$. The analysis is based on a sample of 5.2 pb^{-1} collected in September 2010 at the pp Large Hadron Collider at CERN, at a centre-of-mass energy of $\sqrt{s} = 7 \text{ TeV}$. The contributions from prompt J/ψ and J/ψ from b are separated using the J/ψ pseudo-proper time.

Kruger 2010: Workshop on Discovery Physics at the LHC

December 5 - 10, 2010

Kruger National Park, Mpumalanga, South Africa

^{*}Speaker.

[†]For the LHCb Collaboration.

1. Introduction

This article presents the measurement with the LHCb detector of the production cross-section of prompt J/ψ and J/ψ from b as a function of the J/ψ transverse momentum p_T and rapidity y . Three major sources of J/ψ production in pp collisions can be distinguished: direct J/ψ production, feed-down J/ψ from other heavier charmonium states produced promptly, like $\chi_c \rightarrow J/\psi \gamma$ decays and J/ψ from b -hadron decays. In the following, the first two sources will be called “prompt J/ψ ” and the third one “ J/ψ from b ”. The analysis will lead to a measurement of the production cross-sections $\sigma(\text{prompt } J/\psi, p_T < 14 \text{ GeV}/c, 2 < y < 4.5)$ and $\sigma(J/\psi \text{ from } b, p_T < 14 \text{ GeV}/c, 2 < y < 4.5)$ in pp collisions at $\sqrt{s} = 7 \text{ TeV}$.

2. The LHCb detector and dataset

The study reported here uses 5.2 pb^{-1} of pp collision data recorded by the LHCb experiment at the Large Hadron Collider (LHC) at a centre-of-mass energy of 7 TeV in September 2010.

The LHCb detector is a forward spectrometer described in detail in [1]. All detectors were fully operational and in a stable condition for the data that are included in this analysis. The data were collected using two Level 0 (L0) trigger lines: the single-muon line, which requires one muon candidate with a p_T larger than $1.4 \text{ GeV}/c$, and the dimuon line, which requires two muon candidates with p_T larger than $0.56 \text{ GeV}/c$ and $0.48 \text{ GeV}/c$, respectively. They provide the input candidates for the corresponding High Level Trigger 1 (HLT1) lines: the first one confirms the single-muon candidates from L0, and applies a harder p_T selection at $1.8 \text{ GeV}/c$; the second line confirms the dimuon candidates and requires their combined mass to be greater than $2.5 \text{ GeV}/c^2$. The HLT2 algorithm selects events having two muon candidates with an invariant mass greater than $2.9 \text{ GeV}/c^2$. For a fraction of the data, corresponding to an integrated luminosity of 3.0 pb^{-1} , the HLT1 single muon line was pre-scaled by a factor of five.

To avoid the possibility that a few events with a high occupancy dominate the HLT CPU time, a set of global event cuts (GEC) is applied on the hit multiplicities of each sub-detector used by the pattern recognition algorithms. These cuts were introduced to cope with conditions encountered during the 2010 running period of the LHC, in which the average number of visible interactions per bunch crossing was a factor of five above the design value. The GEC were chosen to reject busy events with a large number of pile-up interactions with minimal loss of luminosity.

3. J/ψ selection

The analysis selects events in which at least one primary vertex is reconstructed. J/ψ candidates are formed from pairs of opposite sign tracks reconstructed in the full tracking system. Each track must have p_T above $0.7 \text{ GeV}/c$, have a good quality of the track fit ($\chi^2/\text{ndf} < 4$) and be identified as a muon. The two muons are required to originate from a common vertex, and only candidates with a χ^2 probability of the vertex fit larger than 0.5% are kept.

J/ψ from b tend to be produced away from the primary vertex and can be separated from prompt J/ψ , which are produced at the primary vertex, by exploiting the J/ψ pseudo-proper time

defined as

$$t_z = \frac{(z_{J/\psi} - z_{PV}) \times M_{J/\psi}}{p_z}, \quad (3.1)$$

where $z_{J/\psi}$ and z_{PV} are the positions along the z -axis of the J/ψ decay vertex and of the primary vertex; p_z is the measured J/ψ momentum in the z direction and $M_{J/\psi}$ the nominal J/ψ mass.

4. Cross-section determination

The differential cross-section for J/ψ production in a given (p_T, y) bin is defined as

$$\frac{d^2\sigma}{dy dp_T} = \frac{N(J/\psi \rightarrow \mu^+\mu^-)}{\mathcal{L} \times \epsilon_{\text{tot}} \times \mathcal{B}(J/\psi \rightarrow \mu^+\mu^-) \times \Delta y \times \Delta p_T}, \quad (4.1)$$

where $N(J/\psi \rightarrow \mu^+\mu^-)$ is the number of observed $J/\psi \rightarrow \mu^+\mu^-$ in bin (p_T, y) , ϵ_{tot} the J/ψ detection efficiency including acceptance and trigger efficiency in bin (p_T, y) , \mathcal{L} the integrated luminosity, $\mathcal{B}(J/\psi \rightarrow \mu^+\mu^-)$ the branching fraction of the $J/\psi \rightarrow \mu^+\mu^-$ decay $((5.93 \pm 0.06) \times 10^{-2}$ [2]), and $\Delta y = 0.5$ and $\Delta p_T = 1 \text{ GeV}/c$ the y and p_T bin sizes, respectively.

In each bin of p_T and y , the number of signal J/ψ from all sources is estimated from an extended unbinned maximum likelihood fit to the invariant mass distribution of the reconstructed J/ψ candidates, where the signal is described by a Crystal Ball function [3] and the combinatorial background by an exponential function. The fraction of J/ψ from b is then extracted from a fit to the t_z distribution. As an example, Fig. 1 (left) shows the mass distribution together with the fit results for one specific bin ($3 < p_T < 4 \text{ GeV}/c$, $2.5 < y < 3.0$). Summing over all bins, a total signal yield of 565 000 events is obtained.

4.1 Determination of the fraction of J/ψ from b

The fraction of J/ψ from b is determined from the fits to the pseudo-proper time t_z and the $\mu^+\mu^-$ invariant mass in each bin of p_T and y . The signal proper-time distribution is described

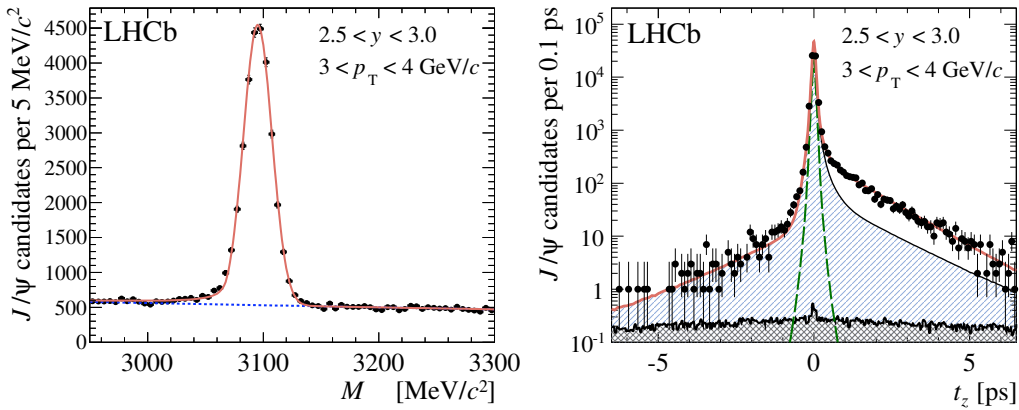


Figure 1: Dimuon mass distribution (left) and t_z distribution (right), with fit results superimposed, for one bin ($3 < p_T < 4 \text{ GeV}/c$, $2.5 < y < 3.0$). On the t_z distribution, the solid red line is the total fit function described in the text, the green dashed line is the prompt J/ψ contribution, the single-hatched area is the background component and the cross-hatched area is the tail contribution.

by a delta function at $t_z = 0$ for the prompt J/ψ component, an exponential decay function for the J/ψ from b component and a long tail arising from the association of the J/ψ candidate with the wrong primary vertex. Since the tail distribution affects the measurement of the J/ψ from b component, a method has been developed to extract its shape from data. The method consists of associating a J/ψ from a given event with the primary vertex of the next event in the J/ψ sample. This simulates the position of an uncorrelated primary vertex with which the J/ψ is associated.

The prompt and b components of the signal function are convolved with a double-Gaussian resolution function. The background consists of random combinations of muons from semi-leptonic b and c decays, which tend to produce positive t_z values, as well as of mis-reconstructed tracks from decays in flight of kaons and pions which contribute both to positive and negative t_z values. The background distribution is parameterised with an empirical function based on the shape of the t_z distribution seen in the J/ψ mass sidebands. It is taken as the sum of a delta function and five exponential components (three for positive t_z and two for negative t_z , the negative and positive exponentials with the largest lifetimes having their lifetimes fixed to the same value), convolved with the sum of two Gaussian functions.

The total fit function is the sum of the products of the mass and t_z fit functions for the signal and background. As an example, Fig. 1 (right) represents the t_z distribution for one specific bin ($3 < p_T < 4$ GeV/ c , $2.5 < y < 3.0$) with the fit result superimposed.

4.2 Efficiency calculation

A simulated sample of inclusive, unpolarised J/ψ mesons is used to estimate the total efficiency ϵ_{tot} in each bin of p_T and y . The total efficiency is the product of the geometrical acceptance, the detection, reconstruction and selection efficiencies, and the trigger efficiency. The efficiencies are assumed to be equal for prompt J/ψ and J/ψ from b in a given (p_T, y) bin because neither the trigger nor the selection makes use of impact parameter or decay length information. A correction to the efficiency is applied to take into account the effect of the global event cuts, introduced during data taking to remove high multiplicity events. The effect of such cuts is estimated from data and found to be equal to $(93 \pm 2)\%$.

4.3 Effect of the J/ψ polarisation on the efficiency

The efficiency is evaluated from a Monte Carlo simulation in which the J/ψ is produced unpolarised. However, studies show that non-zero J/ψ polarisation may lead to very different efficiencies. In this analysis, the efficiency variation is studied in the helicity frame [4].

The angular distribution of the μ^+ from the J/ψ decay is

$$\frac{d^2N}{d\cos\theta d\phi} \propto 1 + \lambda_\theta \cos^2\theta + \lambda_{\theta\phi} \sin 2\theta \cos\phi + \lambda_\phi \sin^2\theta \cos 2\phi, \quad (4.2)$$

where θ is defined as the angle between the direction of the μ^+ momentum in the J/ψ centre-of-mass frame and the direction of the J/ψ momentum in the centre-of-mass frame of the colliding protons, and ϕ is the azimuthal angle measured with respect to the production plane formed by the momenta of the colliding protons in the J/ψ rest frame. When $\lambda_\phi = 0$ and $\lambda_{\theta\phi} = 0$, the values $\lambda_\theta = +1, -1, 0$ correspond to fully transverse, fully longitudinal, and no polarisation, respectively, which are the three default polarisation scenarios considered in this analysis.

The polarisation significantly affects the acceptance and reconstruction efficiencies. The relative efficiency change for prompt J/ψ varies between 3% and 30% depending on p_T and y , when comparing to the unpolarised case. Therefore, the measurement of the differential prompt J/ψ cross-section will be given for the three default polarisations and a separate uncertainty due to the polarisation will be assigned to the integrated cross-section.

5. Systematic uncertainties

The different contributions to the systematic uncertainties affecting the cross-section measurement are discussed in the following and summarised in Table 1.

6. Results

The measured double-differential cross-sections for prompt J/ψ and J/ψ from b in the various (p_T, y) bins, after all corrections and assuming no polarisation, are displayed in Figs. 2. The results for full transverse and full longitudinal polarisation of the J/ψ in the helicity frame are given in Fig. 3. The integrated cross-section for prompt J/ψ production in the defined fiducial region, summing over all bins of the analysis, is

$$\sigma(\text{prompt } J/\psi, p_T < 14 \text{ GeV}/c, 2.0 < y < 4.5) = 10.52 \pm 0.04 \pm 1.40^{+1.64}_{-2.20} \mu\text{b}, \quad (6.1)$$

Table 1: Summary of systematic uncertainties.

Source	Systematic uncertainty (%)
<i>Correlated between bins</i>	
Inter-bin cross-feed	0.5
Mass fits	1.0
Radiative tail	1.0
Muon identification	1.1
Tracking efficiency	8.0
Track χ^2	1.0
Vertexing	0.8
GEC	2.0
$\mathcal{B}(J/\psi \rightarrow \mu^+ \mu^-)$	1.0
Luminosity	10.0
<i>Uncorrelated between bins</i>	
Bin size	0.1 to 15.0
Trigger	1.7 to 4.5
<i>Applied only to J/ψ from b cross-sections, correlated between bins</i>	
GEC efficiency on B events	2.0
t_z fits	3.6

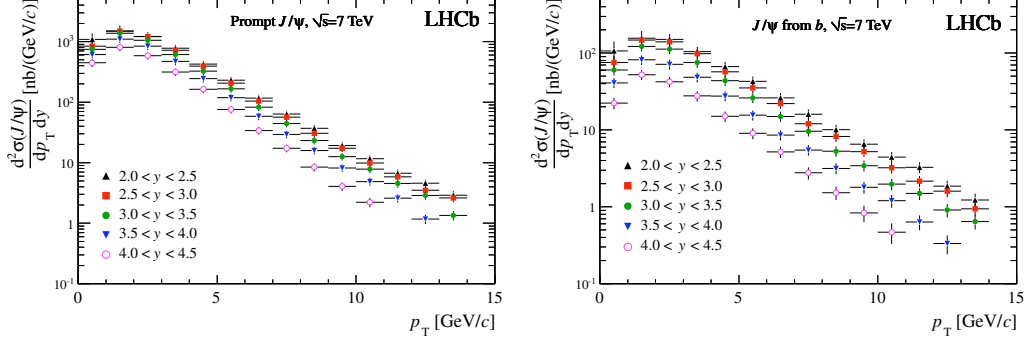


Figure 2: Differential production cross-section for prompt J/ψ (left) and J/ψ from b (right) as a function of p_T in bins of y , assuming that prompt J/ψ are produced unpolarised. The errors are the quadratic sums of the statistical and systematic uncertainties.

where the first uncertainty is statistical and the second systematic. The result is quoted assuming unpolarised J/ψ and the last error indicates the uncertainty related to this assumption. The integrated cross-section for the production of J/ψ from b in the same fiducial region is

$$\sigma(J/\psi \text{ from } b, p_T < 14 \text{ GeV}/c, 2.0 < y < 4.5) = 1.14 \pm 0.01 \pm 0.16 \mu\text{b}, \quad (6.2)$$

where the first uncertainty is statistical and the second systematic.

References

- [1] The LHCb Collaboration, A. A. Alves *et al.*, JINST **3** (2008) S08005.
- [2] The Particle Data Group, K. Nakamura *et al.*, J. Phys. G **37** (2010) 075021.
- [3] J. E. Gaiser, Ph.D. Thesis, [SLAC-R-255](#) (1982); T. Skwarnicki, Ph.D. Thesis, [DESY-F31-86-02](#) (1986).
- [4] K. Gottfried and J. D. Jackson, Nuovo Cimento **33** (1964) 309; C. S. Lam and W.-K. Tung, Phys. Rev. D **18** (1978) 2447.

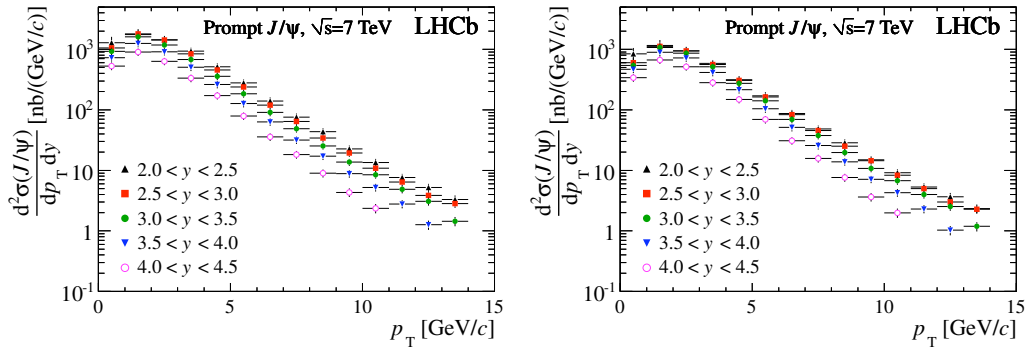


Figure 3: Differential production cross-section for prompt J/ψ as a function of p_T in bins of y , assuming full transverse (left) or full longitudinal (right) J/ψ polarisation. The errors are the quadratic sums of the statistical and systematic uncertainties.